Journal of Sound and Vibration (2002) **256**(3), 499–513
doi:10.1006/jsvi.5002, available online at http://www.idealibrary.com on IDEAL®

OPTIMAL DAMPING OF STAYS IN CABLE-STAYED BRIDGES FOR IN-PLANE VIBRATIONS

C. N. JENSEN

ES-Consult, Ltd., Staktoften 20, DK-2950 Vedbæk, Denmark

AND

S. R. K. NIELSEN AND J. D. SØRENSEN

Department of Building Technology and Structural Engineering, Aalborg University, Sohngaardsholmvej 57, DK-9000, Aalborg, Denmark. E-mail: soren.nielsen@civil.auc.dk

(*Received* 17 *May* 2000, *and in final form* 15 *February* 2001)

Significant vibrations have been reported in stays of recently constructed cable stayed bridges. The vibrations appear as in-plane vibrations that may be caused by rain–wind-induced aeroelastic interaction or by resonance excitation of the cables from the motion of the pylons. The stays of modern cable-stayed bridges are often designed as twin cables with a spacing of, say 1 m. In such cases, it is suggested in the paper to suppress the mentioned in-plane types of vibrations by means of a tuned mass–damper (TMD) placed between the twin cables at their midpoints. The TMD divides the stay into four half-cables, and resonance may occur in each of the half-cables as well as in the entire stay. The optimal tuning of the TMD is investigated based on a mathematical model, where the motion of the support points on the pylons is considered to be the main cause of excitation. The indicated motion is modelled as a band-limited Gaussian white noise process. Three load scenarios are considered: narrow-banded excitations, with the central frequency of the autospectrum close to the lowest eigenfrequency of each of the two cables constituting the stay, and a broadbanded excitation which encompasses both of the mentioned frequencies. The spring and the damper constants of the TMD are optimized so that the variances of the displacement of the adjacent four half-cables, the support point of the TMD and the secondary mass are minimized. At optimal design, it is shown that the variances reduce below 14% of those of the unprotected stay.

1. INTRODUCTION

The application of cables for support of structures has found increasing use for example as stay cables for towers and bridges, see reference [1]. Due to the slenderness of cables and the very low internal damping in them, cables are prone to vibrations.

Unacceptable oscillations of the cables in stayed bridges have appeared on several occasions, some of which are mentioned here as examples: the Farø Bridge in Denmark, the Erasmus Bridge in Rotterdam, the Köhlbrand Bridge in Hamburg, Germany, etc. The occurrence of oscillations of the stay cables may lead to corrosion of strands or even fatigue failure. The failures of cables in the Saint-Nazaire bridge in France and the Zarate Brazo Largo bridge in Argentina are believed to be caused by fatigue due to cable vibrations, see reference [2].

Various phenomena can generate the cable vibrations. For example, vortex shedding, different galloping phenomena, wind-induced vibration, and rain–wind-induced vibrations. Especially, the subject of rain–wind-induced cable vibrations has recently received extensive

0022-460X/02/$35.00

attention, see reference [3]. These appear as in-plane vibrations and are assumed to be initiated by migrating rivulets on the wet surface of the cable. Another source considered is the motion of the cable support point resulting in harmonic or parametric resonance as the driving mechanism for the vibrations [4].

To reduce oscillation problems different means have been applied. Often these aim at increasing the internal damping of the stays, e.g., by installation of hydraulic dampers between the stay and the bridge girder. At some places, the stays have been interconnected by ropes thereby increasing the damping and changing the resonance frequencies.

In this paper, stays consisting of twin cables and a tuned mass–damper (TMD) for minimizing the in-plane vibrations are considered. In stayed bridges, cables with a variety of circular eigenfrequencies are present due to the variable lengths of the cables. Hence some cables are likely to be exposed to resonance from the support point motion of the pylons, which are essentially narrowbanded in nature with a central frequency reflecting the fundamental eigenfrequency of the bridge. At the newly constructed cable-stayed Øresund Bridge connecting Sweden and Denmark, for which twin cables were adopted, it was considered to use TMDs placed between the twin cables to limit the vibrations of the cables in stays which were likely to resonance excitation. The paper addresses the basic research performed in this connection, and clearly demonstrates the applicability of the idea. It should be noted that for the Øresund bridge, the idea was finally abandoned for practical reasons. Since a TMD can only be expected to work when tuned to a single frequency, it was the choice of the authors to optimize the TMD primarily to narrowbanded excitation with a central frequency equal to the lowest eigenfrequencies of the cable.

The non-linear modal restoring forces due to support-point motions involve primarily cubic geometrical non-linearities in combination to a linear parametric term. In case of harmonic resonant excitation, the parametric term will not affect the first order perturbational solution of the harmonic response [5]. For moderate amplitudes, the response to an in-plane excitation is in plane. A critical level exists, however, such that the dominating response bifurcates to a whirling motion, where the in-plane and out-of-plane components have same frequency. By contrast, the superharmonic case of order 2, i.e., with excitation frequency equal to half the fundamental eigenfrequency, is driven primarily by the parametric term [5]. The response is primarily in-plane with a transition to a whirling motion bifurcating from the in plane motion at a critical response level, quite similar to the harmonic response case. Since the superharmonic vibration frequency is in the vicinity of the lowest eigenfrequencies of the cable, the TMD tuned at harmonic response is expected to have some effect against these motions too. Subharmonic response of order 2, i.e., where the excitation frequency equals twice the fundamental eigenfrequency of the cable, is also primarily driven by the parametric term. In that case, the response appears as a harmonic in-plane component (with a frequency equal to that of the excitation thus close to twice the eigenfrequency of the cable) coupled to an out-of-plane subharmonic component (with a frequency close to that of the fundamental eigenmode of the cable), resulting in a trajectory of the cable shaped as a horizontal eight [6]. For this reason, a mass–damper active against in-plane vibrations and tuned to the resonance frequencies is not expected to have much effect on the in-plane component, and hence on the combined motion.

In this paper focus is on the harmonic case, i.e., where the frequency of the excitation is close to the fundamental eigenfrequency of the cable. In this case, the TMD is expected to be an effective means against vibrations. It is, therefore, presumed that the non-linearities will not have significant influence on the cable dynamics, and the non-linearity due to vibrations in the cable forces (the parametric term) is of secondary importance and is excluded in the formulation. Furthermore, it is assumed that the cables can be described as linear elastic and perfectly flexible in bending. As described above, though, the results in this paper also

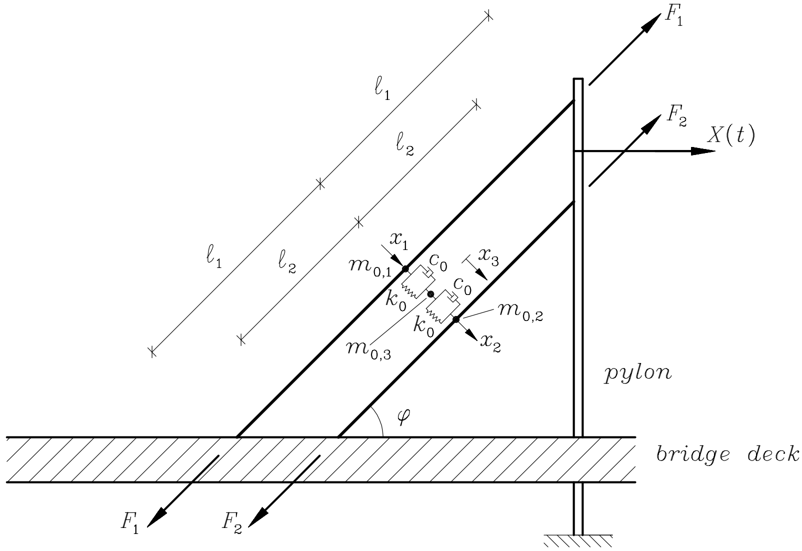

Figure 1. Model for cables and damper.

have relevance for other types of driving mechanisms for the vibrations, depending on the method for optimization of the TMD, and could be used as the means for increasing the overall damping of the cable system.

The presence of the TMD between the midpoints of the two cables results in discontinuities in the slopes of the cables. Therefore, equations of motion are set up for the half-cables and an extra degree of freedom is introduced at the cable midpoints. We then end up with a discretized system of seven coupled second order differential equations as equations of motion, see Section 2. To determine the optimal TMD characteristics, two alternative optimization problems are formulated in Section 3. Numerical illustrations of the model are presented in Section 4.

2. MODELLING OF DYNAMIC BEHAVIOUR OF COUPLED STAYS

Each stay is assumed to be composed of two cables typically spaced, say 1 m, as shown in Figure 1. It is assumed that a TMD is established between the midpoint of the two cables. The TMD consists of two springs with stiffness k_0 and two dampers with damping coefficient c_0. The total mass m_0 of the TMD is divided into three concentrated masses $m_{0,1} = \alpha_m m_0$, $m_{0,2} = \alpha_m m_0$ and $m_{0,3} = (1 - 2\alpha_m)\, m_0$, where the coefficient α_m, $0 \leq \alpha_m \leq 0{\cdot}5$ models the distribution of the TMD mass.

The displacements of the three degrees of freedom indicated in Figure 1 are denoted x_1, x_2 and x_3, and the corresponding masses are $m_{0,1}$, $m_{0,2}$ and $m_{0,3}$. $X(t)$ is the forced displacement of the pylon (and thus the two cables). Further, the non-straightness of the vibrating cables is taken into account by introducing an extra degree of freedom for each of the four half-cables (see below).

The static deflections for the two cables in the degrees of freedom x_1 and x_2 become

$$u_1 = \frac{[2(F_2/l_2)\, m_1 + \frac{1}{2} k_0 (m_1 + m_2)]}{[4(F_1/l_1)(F_2/l_2) + k_0(F_1/l_1 + F_2/l_2)]}\, g \cos\varphi, \tag{1}$$

$$u_2 = \frac{[2(F_1/l_1)\, m_2 + \frac{1}{2} k_0 (m_1 + m_2)]}{[4(F_1/l_1)(F_2/l_2) + k_0(F_1/l_1 + F_2/l_2)]}\, g \cos\varphi, \tag{2}$$

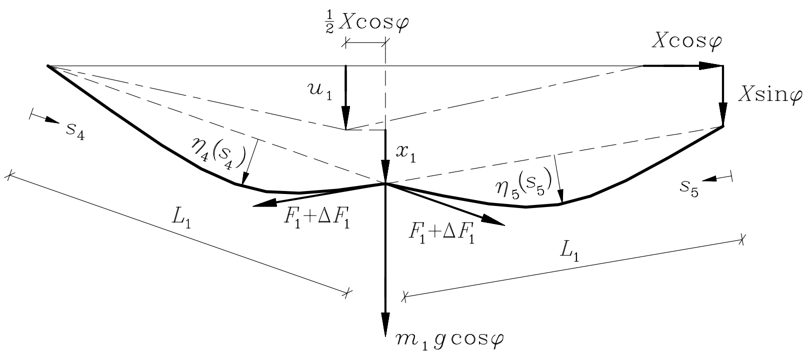

Figure 2. Geometrical deformation for dynamic cable analysis.

where F_j is the force in cable no j, l_j is half the length of cable no. j, g is the acceleration of gravity and m_j is the mass allocated to the jth cable:

$$m_j = \tfrac{1}{2}\, m_{0,j} + \mu l_j, \quad j = 1, 2, \tag{3}$$

where μ is the mass per unit length of the cables. The increase in cable force ΔF_j due to an increment Δl_j of the cable length is

$$\Delta F_j = AE_j \frac{\Delta l_j}{2l_j}, \quad j = 1, 2. \tag{4}$$

EA_j is the axial stiffness for cable j. The total extension Δl_j of cable no. j is determined considering the static deformation of the cable. Neglecting second order terms, Δl_j is approximately given by (see Figure 2)

$$\Delta l_j \simeq X\cos\varphi - \frac{u_j}{l_j} X\sin\varphi + 2\frac{u_j}{l_j} x_j, \quad j = 1, 2. \tag{5}$$

The dynamic vibrations of each half-cable is assumed to be described by a single-degree-of-freedom (s.d.o.f.) modal expansion. For cable no. 1, the displacements η_4 and η_5 of the two half-cables in the transverse direction are represented by the following single-mode approximation:

$$\eta_i(s_i, t) = x_i(t)\sin\left(\pi \frac{s_i}{L_1}\right), \quad i = 4, 5, \tag{6}$$

where s_i is a co-ordinate along the deformed chord of the length $L_1 = l_1 + \Delta l_1$. The modal co-ordinates $x_4(t)$ and $x_5(t)$ can be considered as the relative displacements of the half-cables at their midpoints. Hence, $x_4(t)$ and $x_5(t)$ have dimension of length.

The equations of vibration of the half-cables 4 and 5 become

$$(F_1 + \Delta F_1)\frac{\partial^2 \eta_4}{\partial s_4^2} - \mu\left(\ddot{\eta}_4 + \ddot{x}_1 \frac{s_4}{L_1}\right) = 0, \tag{7}$$

$$(F_1 + \Delta F_1)\frac{\partial^2 \eta_5}{\partial s_5^2} - \mu\left(\ddot{\eta}_5 + \ddot{x}_1 \frac{s_5}{L_1} + \ddot{X}\left(1 - \frac{s_5}{L_1}\right)\sin\varphi\right) = 0. \tag{8}$$

The corresponding linearized modal co-ordinate equations become

$$\ddot{x}_4 + \frac{F_1}{\mu l_1^2}\pi^2 x_4 + \frac{2}{\pi}\ddot{x}_1 = 0, \tag{9}$$

$$\ddot{x}_5 + \frac{F_1}{\mu l_1^2}\pi^2 x_5 + \frac{2}{\pi}(\ddot{x}_1 + \ddot{X}\sin\varphi) = 0. \tag{10}$$

Similar expressions are derived for the half-cables 6 and 7 in cable no. 2.

If the stiffness and damping contributions from the TMD are neglected, the equations of vibration for the two concentrated masses $m_{0,1}$ and $m_{0,2}$ can be written for $|x_j|, |X| \ll u_j$, $j = 1, 2$ (which implies the first order approximation $L_1 \approx l_1$):

$$\begin{aligned} m_{0,1}\ddot{x}_1 &+ (F_1 + \varDelta F_1)\frac{x_1 + u_1}{l_1} + \int_0^{l_1} \frac{s}{l_1}\mu\left(\ddot{\eta}_4 + \ddot{x}_1\frac{s}{l_1}\right)\mathrm{d}s \\ &+ (F_1 + \varDelta F_1)\frac{(x_1 + u_1 - X\sin\varphi)}{l_1} \\ &+ \int_0^{l_1} \frac{s}{l_1}\mu\left(\ddot{\eta}_5 + \ddot{x}_1\frac{s}{l_1} + \ddot{X}\left(1 - \frac{s}{l_1}\right)\sin\varphi\right)\mathrm{d}s = m_1 g\cos\varphi, \end{aligned} \tag{11}$$

$$\begin{aligned} m_{0,2}\ddot{x}_2 &+ (F_2 + \varDelta F_2)\frac{x_2 + u_2}{l_2} + \int_0^{l_2} \frac{s}{l_2}\mu\left(\ddot{\eta}_6 + \ddot{x}_2\frac{s}{l_2}\right)\mathrm{d}s \\ &+ (F_2 + \varDelta F_2)\frac{(x_2 + u_2 - X\sin\varphi)}{l_2} \\ &+ \int_0^{l_2} \frac{s}{l_2}\mu\left(\ddot{\eta}_7 + \ddot{x}_2\frac{s}{l_2} + \ddot{X}\left(1 - \frac{s}{l_2}\right)\sin\varphi\right)\mathrm{d}s = m_2 g\cos\varphi, \end{aligned} \tag{12}$$

where the second and fourth terms in equations (11) and (12), respectively, are the projections of the cable forces on vertical from right and left half-cable, respectively, whereas the third and fifth terms represent the reactions on vertical at x_1 and x_2, from the inertial loads on half-cables 4 and 5, and 6 and 7 respectively. The third and fifth terms are found as the moments of the inertial forces about x_1 and x_2.

Using equations (3)–(7), linearization implies the following equations of vibration:

$$\begin{aligned} m_{0,1}\ddot{x}_1 &+ 2\left(\frac{F_1}{l_1} + \frac{AE_1}{l_1}\left(\frac{u_1}{l_1}\right)^2\right)x_1 - \pi\frac{F_1}{l_1}(x_4 + x_5) \\ &= \left[\left(\frac{F_1}{l_1} + \frac{AE_1}{l_1}\left(\frac{u_1}{l_1}\right)^2\right)\sin\varphi - \frac{AE_1}{l_1}\frac{u_1}{l_1}\cos\varphi\right]X(t), \end{aligned} \tag{13}$$

$$m_{0,2}\ddot{x}_2 + 2\left(\frac{F_2}{l_2} + \frac{AE_2}{l_2}\left(\frac{u_2}{l_2}\right)^2\right)x_2 - \pi\frac{F_2}{l_2}(x_6 + x_7)$$

$$= \left[\left(\frac{F_2}{l_2} + \frac{AE_2}{l_2}\left(\frac{u_2}{l_2}\right)^2\right)\sin\varphi - \frac{AE_2}{l_2}\frac{u_2}{l_2}\cos\varphi\right]X(t). \tag{14}$$

Introducing structural damping in the half-cables by the linear viscous modal damping coefficient c_1, the following equations of motion for the cables are obtained with the damping and stiffness forces from the TMD added:

$$m_{0,1}\ddot{x}_1 + c_0(\dot{x}_1 - \dot{x}_3) + 2\left(\frac{F_1}{l_1} + \frac{AE_1}{l_1}\left(\frac{u_1}{l_1}\right)^2\right)x_1$$

$$- \pi\frac{F_1}{l_1}(x_4 + x_5) + k_0(x_1 - x_3)$$

$$= \left[\left(\frac{F_1}{l_1} + \frac{AE_1}{l_1}\left(\frac{u_1}{l_1}\right)^2\right)\sin\varphi - \frac{AE_1}{l_1}\frac{u_1}{l_1}\cos\varphi\right]X(t), \tag{15}$$

$$m_{0,2}\ddot{x}_2 + c_0(\dot{x}_2 - \dot{x}_3) + 2\left(\frac{F_2}{l_2} + \frac{AE_2}{l_2}\left(\frac{u_2}{l_2}\right)^2\right)x_2$$

$$- \pi\frac{F_2}{l_2}(x_6 + x_7) + k_0(x_2 - x_3)$$

$$= \left[\left(\frac{F_2}{l_2} + \frac{AE_2}{l_2}\left(\frac{u_2}{l_2}\right)^2\right)\sin\varphi - \frac{AE_2}{l_2}\frac{u_2}{l_2}\cos\varphi\right]X(t), \tag{16}$$

$$m_{0,3}\ddot{x}_3 + c_0(2\dot{x}_3 - \dot{x}_1 - \dot{x}_2) + k_0(2x_3 - x_1 - x_2) = 0, \tag{17}$$

$$\ddot{x}_4 + \frac{F_1}{\mu l_1^2}\pi^2 x_4 + c_1\dot{x}_4 + \frac{2}{\pi}\ddot{x}_1 = 0, \tag{18}$$

$$\ddot{x}_5 + \frac{F_1}{\mu l_1^2}\pi^2 x_5 + c_1\dot{x}_5 + \frac{2}{\pi}(\ddot{x}_1 + \ddot{X}\sin\varphi) = 0, \tag{19}$$

$$\ddot{x}_6 + \frac{F_2}{\mu l_2^2}\pi^2 x_6 + c_1\dot{x}_6 + \frac{2}{\pi}\ddot{x}_2 = 0, \tag{20}$$

$$\ddot{x}_7 + \frac{F_2}{\mu l_2^2}\pi^2 x_7 + c_1\dot{x}_7 + \frac{2}{\pi}(\ddot{x}_2 + \ddot{X}\sin\varphi) = 0. \tag{21}$$

Next, the motion of the pylon is assumed to vary harmonically with time at the circular vibration frequency ω, i.e.,

$$X(t) = \exp(\mathrm{i}\omega t). \tag{22}$$

The complex amplitude $X_1(\omega), \ldots, X_7(\omega)$ of the selected d.o.f. can be considered as frequency response functions and is then determined from the following system of linear equations:

$$\mathbf{X}(\omega) = \mathbf{H}(\omega)\mathbf{b}, \tag{23}$$

where $\mathbf{H}(\omega)$ signifies the frequency response matrix of the system.

$$\mathbf{X}(\omega) = \begin{bmatrix} X_1(\omega) \\ X_2(\omega) \\ \vdots \\ X_7(\omega) \end{bmatrix}, \tag{24}$$

$$\mathbf{H}(\omega) = (-\omega^2\mathbf{M} + \mathrm{i}\omega\mathbf{C} + \mathbf{K})^{-1}, \tag{25}$$

where $\mathbf{M}$ is the mass matrix, $\mathbf{C}$ is the damping matrix and $\mathbf{K}$ is the stiffness matrix given by

$$\mathbf{M} = \begin{bmatrix} m_{0,1} & 0 & 0 & 0 & 0 & 0 & 0 \\ 0 & m_{0,2} & 0 & 0 & 0 & 0 & 0 \\ 0 & 0 & m_{0,3} & 0 & 0 & 0 & 0 \\ \frac{2}{\pi} & 0 & 0 & 1 & 0 & 0 & 0 \\ \frac{2}{\pi} & 0 & 0 & 0 & 1 & 0 & 0 \\ 0 & \frac{2}{\pi} & 0 & 0 & 0 & 1 & 0 \\ 0 & \frac{2}{\pi} & 0 & 0 & 0 & 0 & 1 \end{bmatrix}, \tag{26}$$

$$\mathbf{C} = \begin{bmatrix} c_0 & 0 & -c_0 & 0 & 0 & 0 & 0 \\ 0 & c_0 & -c_0 & 0 & 0 & 0 & 0 \\ -c_0 & -c_0 & 2c_0 & 0 & 0 & 0 & 0 \\ 0 & 0 & 0 & c_1 & 0 & 0 & 0 \\ 0 & 0 & 0 & 0 & c_1 & 0 & 0 \\ 0 & 0 & 0 & 0 & 0 & c_1 & 0 \\ 0 & 0 & 0 & 0 & 0 & 0 & c_1 \end{bmatrix}, \tag{27}$$

$$\mathbf{K}=\begin{bmatrix} K_{11} & 0 & -k_0 & -F_1\frac{\pi}{l_1} & -F_1\frac{\pi}{l_1} & 0 & 0 \\ 0 & K_{22} & -k_0 & 0 & 0 & -F_2\frac{\pi}{l_2} & -F_2\frac{\pi}{l_2} \\ -k_0 & -k_0 & 2k_0 & 0 & 0 & 0 & 0 \\ 0 & 0 & 0 & \frac{F_1}{\mu l_1^2}\pi^2 & 0 & 0 & 0 \\ 0 & 0 & 0 & 0 & \frac{F_1}{\mu l_1^2}\pi^2 & 0 & 0 \\ 0 & 0 & 0 & 0 & 0 & \frac{F_2}{\mu l_2^2}\pi^2 & 0 \\ 0 & 0 & 0 & 0 & 0 & 0 & \frac{F_2}{\mu l_2^2}\pi^2 \end{bmatrix}, \tag{28}$$

$$K_{11}=2\left(\frac{F_1}{l_1}+\frac{AE_1}{l_1}\left(\frac{u_1}{l_1}\right)^2\right)+k_0, \tag{29}$$

$$K_{22}=2\left(\frac{F_2}{l_2}+\frac{AE_2}{l_2}\left(\frac{u_2}{l_2}\right)^2\right)+k_0. \tag{30}$$

It is noted that with the chosen degrees of freedom the mass and stiffness matrices are not symmetric. Symmetric equations can be achieved by means of linear operations, e.g., to orthogonal modal co-ordinates, where the equations are diagonalized. Since no gain would be achieved in the analysis from such a co-ordinate transformation, it has not been performed.

The loading vector $\mathbf{b}$ is given by

$$\mathbf{b}=\begin{bmatrix} \left(\frac{F_1}{l_1}+\frac{AE_1}{l_1}\left(\frac{u_1}{l_1}\right)^2\right)\sin\varphi-\frac{AE_1}{l_1}\frac{u_1}{l_1}\cos\varphi \\ \left(\frac{F_2}{l_2}+\frac{AE_2}{l_2}\left(\frac{u_2}{l_2}\right)^2\right)\sin\varphi-\frac{AE_2}{l_2}\frac{u_2}{l_2}\cos\varphi \\ 0 \\ 0 \\ \frac{2\omega^2}{\pi}\sin\varphi \\ 0 \\ \frac{2\omega^2}{\pi}\sin\varphi \end{bmatrix}. \tag{31}$$

3. OPTIMAL DAMPER CHARACTERISTICS

The displacement of the support point of the cable is modelled as a band-limited white noise $\{X(t), t\in R\}$ with the autospectral density $S_X(\omega)$, the variance σ_X^2, the circular central

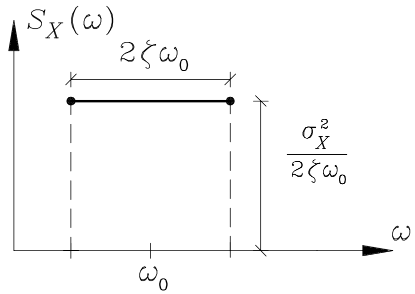

Figure 3. Band limited white noise.

frequency ω_0 and the band width $2\zeta\omega_0$, see Figure 3.

$$S_X(\omega) = \begin{cases} \dfrac{1}{2\zeta\omega_0}\sigma_X^2, & \omega \in [(1-\zeta)\omega_0, \quad (1+\zeta)\omega_0], \\ 0, & \omega \notin [(1-\zeta)\omega_0, \quad (1+\zeta)\omega_0]. \end{cases} \tag{32}$$

The stationary variance of the considered degree of freedom $\{X_j(t)\}$ then becomes, see e.g., reference [7],

$$\sigma_{X_j}^2 = \int_0^\infty |X_j(\omega)|^2 S_X(\omega)\,\mathrm{d}\omega = \frac{\sigma_X^2}{2\zeta\omega_0}\int_{\omega_0(1-\zeta)}^{\omega_0(1+\zeta)} |X_j(\omega)|^2\,\mathrm{d}\omega \tag{33}$$

Three load cases are considered, characterized by specific choices of ω_0 and ζ

$$\begin{aligned} &1\colon \quad \omega_0 = \omega_1, \quad \zeta = 0{\cdot}1, \\ &2\colon \quad \omega_0 = \omega_2, \quad \zeta = 0{\cdot}1, \\ &3\colon \quad \omega_0 = 4s^{-1}, \quad \zeta = 1, \end{aligned} \tag{34}$$

where

$$\omega_1 = \sqrt{\frac{K_{11}}{m_{0,1}}}, \quad \omega_2 = \sqrt{\frac{K_{22}}{m_{0,2}}} \tag{35}$$

signifies the circular eigenfrequencies of the upper and the lower cable respectively. K_{11} and K_{22} are given by equations (29) and (30). Load cases 1 and 2 are narrowbanded excitations with circular central frequencies, which are likely to excite the corresponding eigenmodes. Load case 3 is a broadbanded excitation, which corresponds to both resonance frequencies.

Optimal design of the damper and the distribution of cable forces between cables 1 and 2 can be made with one of the following objectives:

$$\min \sigma_1^2 = \sum_{j=1}^{2} \sigma_{X_j}^2 + \sum_{j=4}^{7} \sigma_{X_j}^2 \tag{36}$$

and/or

$$\min \sigma_2^2 = \sum_{j=1}^{7} \sigma_{X_j}^2. \tag{37}$$

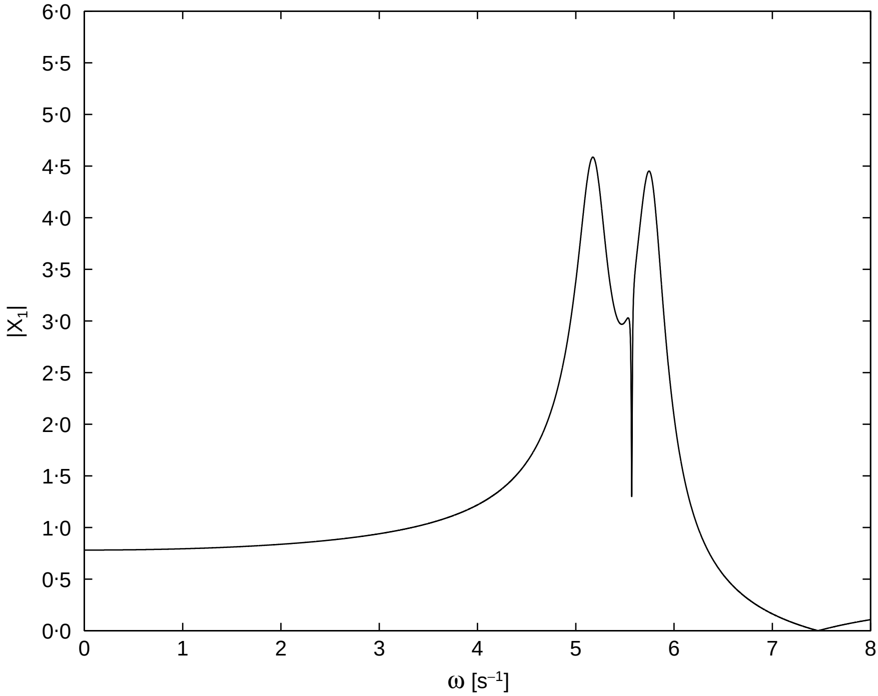

Figure 4. $|X_1(\omega)|$ for $(\alpha_m, \alpha_F, m_0, c_0, k_0) = (0{\cdot}1, \ -0{\cdot}0135, 200\,\text{kg}, \ 50\ \text{Ns/m}, 2350\text{N/m})$.

The objective of equation (36) is the sum of the variances of the displacements of the midpoint of the two cables and the midpoints of the four half-cables. The objective of equation (37) is the sum of the variances of all displacements including the displacement of the TMD.

Generally, constraints can be added to the above optimization problems. Especially, constraints enforcing the eigenfrequencies of the vibration modes of the two coupled cables to be sufficiently different from the vibration frequencies of the pylons are relevant.

The design parameters of the problem are chosen as the spring stiffness k_0 and the damper constant c_0 of the TMD. The distribution of the TMD mass is measured by the parameter α_m, (see section 2). The total cable force $F_1 + F_2$ of the two twin cables is fixed. However, the distribution on the cables may be varied. The distribution of cable forces is measured by a parameter α_F defined by the relation

$$F_2 = (1 + \alpha_F)\,F_1. \tag{38}$$

4. EXAMPLE

The following representative data are used: $l_1 = 85$ m, $l_2 = 84{\cdot}4$ m, $\varphi = 30{\cdot}4°$, $\mu_1 = \mu_2 = 73$ kg/m, $F_2 = (1 + \alpha_F)F_1$ and $F_1 + F_2 = 9{\cdot}7 \times 10^6$ N and $c_1 = 0{\cdot}02$ Ns/m.

In Figures 4–10, $|X_1(\omega)|, \ldots, |X_7(\omega)|$ are shown for $(\alpha_m, \alpha_F, m_0, c_0, k_0) = (0{\cdot}1, \ -0{\cdot}0135,$ 200 kg, 50 Ns/m, 2350 N/m). The resonance frequencies are 5·2 and 5·8 s^{-1}. It should be noted that the unit of the ordinates in Figures 4–10 is the same, such that one can compare the relative vibration level of each of the variables. Since the analysis performed is linear, the

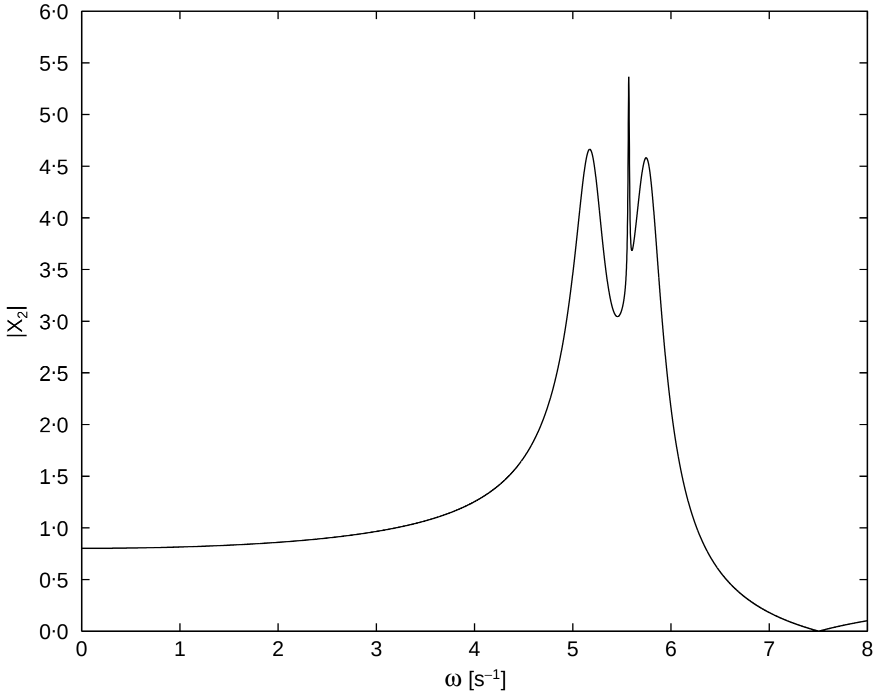

Figure 5. $|X_2(\omega)|$ for $(\alpha_m, \alpha_F, m_0, c_0, k_0) = (0{\cdot}1, \ -0{\cdot}0135, 200\,\mathrm{kg}, 50\ \mathrm{Ns/m}, 2350\ \mathrm{N/m})$.

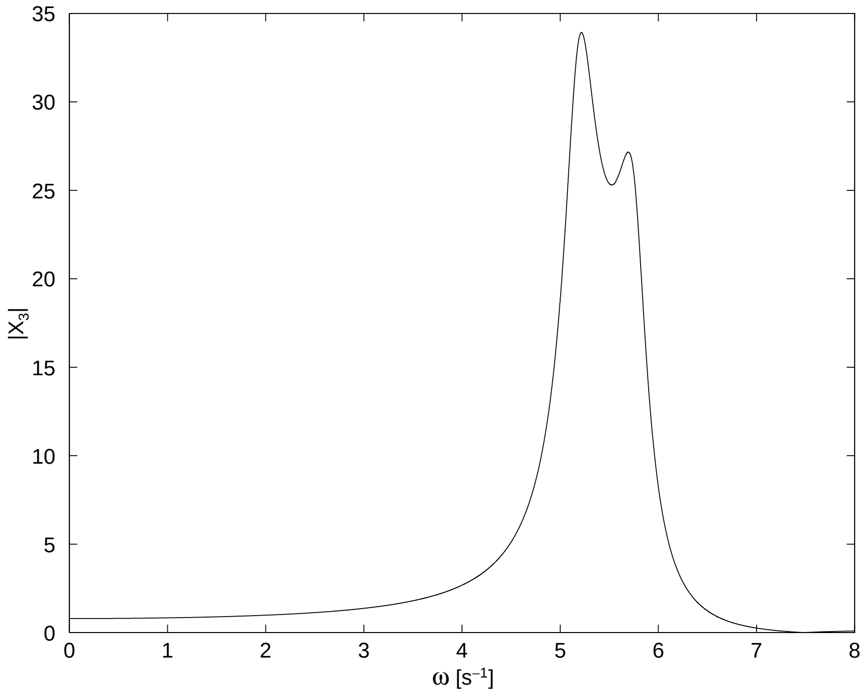

Figure 6. $|X_3(\omega)|$ for $(\alpha_m, \alpha_F, m_0, c_0, k_0) = (0{\cdot}1, \ -0{\cdot}0135, 200\,\mathrm{kg}, 50\,\mathrm{Ns/m}, 2350\ \mathrm{N/m})$.

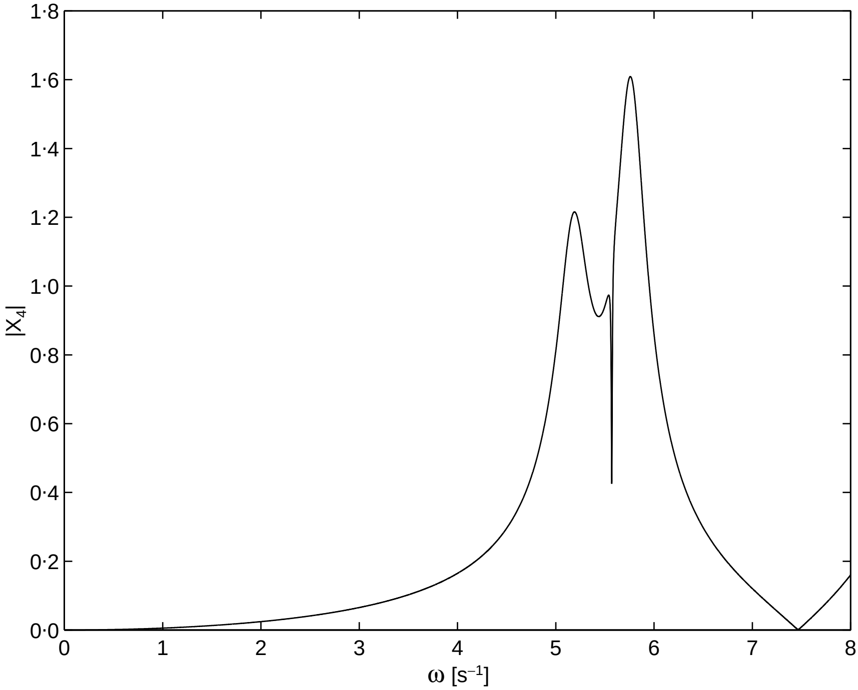

Figure 7. $|X_4(\omega)|$ for $(\alpha_m, \alpha_F, m_0, c_0, k_0) = (0{\cdot}1,\ -0{\cdot}0135$, 200 kg, 50 Ns/m, 2350 N/m).

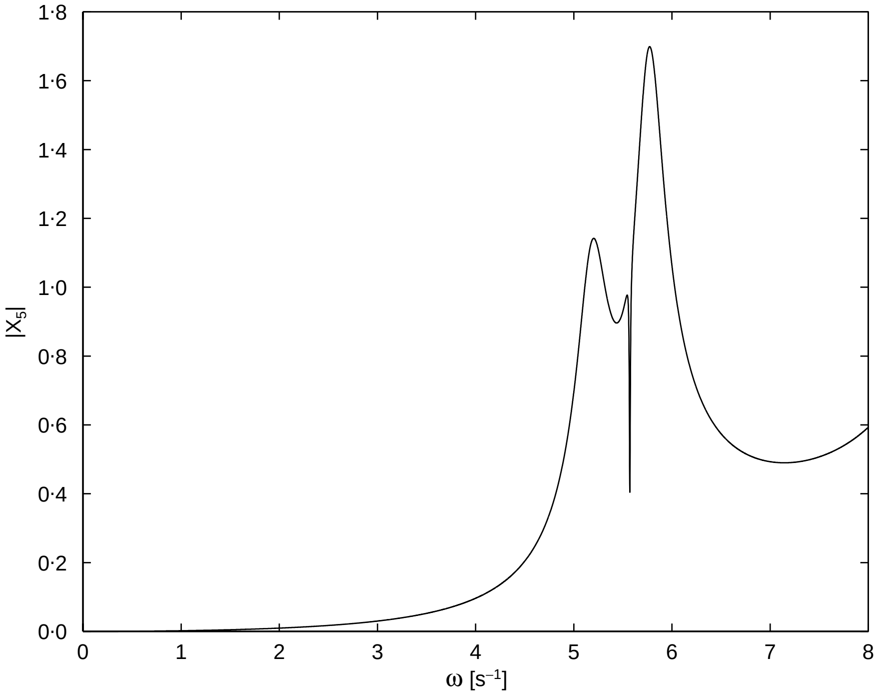

Figure 8. $|X_5(\omega)|$ for $(\alpha_m, \alpha_F, m_0, c_0, k_0) = (0{\cdot}1,\ -0{\cdot}0135$, 200 kg, 50 Ns/m, 2350 N/m).

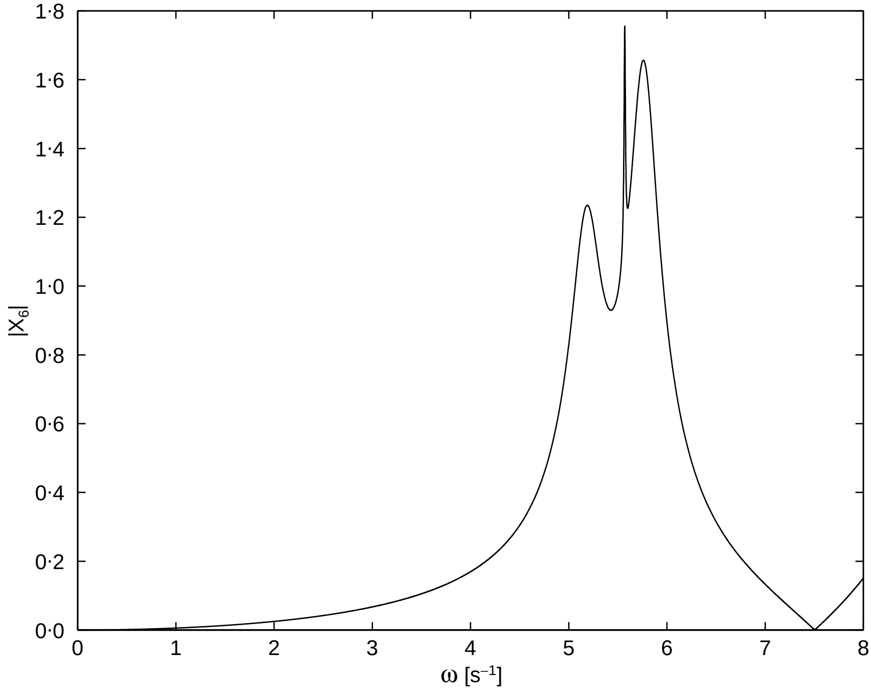

Figure 9. $|X_6(\omega)|$ for $(\alpha_m, \alpha_F, m_0, c_0, k_0) = (0{\cdot}1, -0{\cdot}0135, 200$ kg, 50 Ns/m, 2350 N/m).

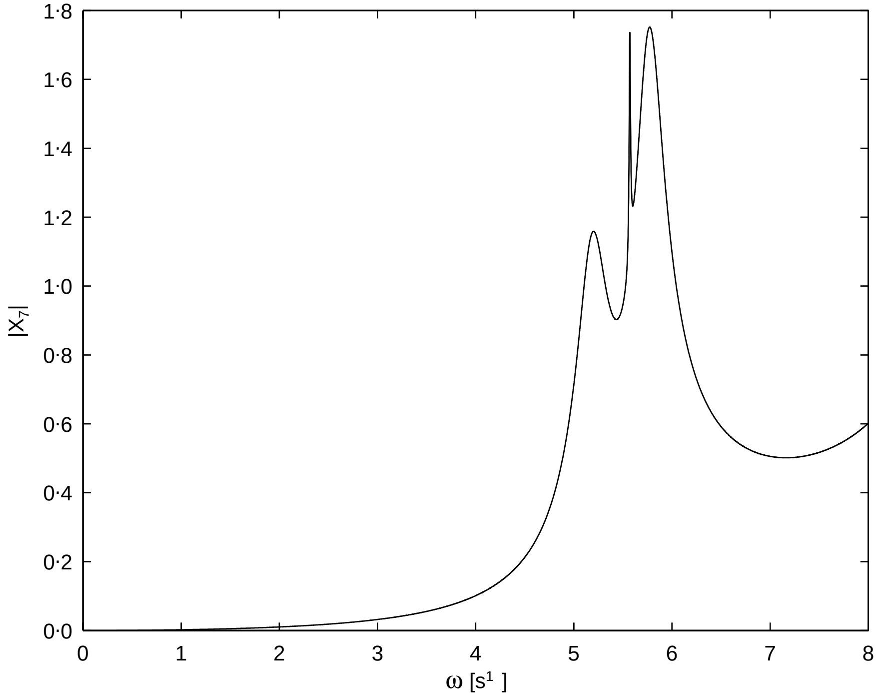

Figure 10. $|X_7(\omega)|$ for $(\alpha_m, \alpha_F, m_0, c_0, k_0) = (0{\cdot}1, -0{\cdot}0135, 200$ kg, 50 Ns/m, 2350 N/m).

TABLE 1

The variances for different optimization objectives

		Spectrum 1		Spectrum 2		Spectrum 3	
k_0	c_0	σ_1^2	σ_2^2	σ_1^2	σ_2^2	σ_1^2	σ_2^2
2350	50	5·85	79·8	5·86	80·1	**0·81**	12·3
1600	210	3·59	9·1	3·60	9·16	2·20	**4·04**
1200	15	**2·89**	53·8	**2·90**	53·8	13·5	20·8

absolute value of the ordinates is irrelevant and has been omitted from the figures. It is seen that the influence of the TMD is significant in the frequency interval from 4 to 7 s^{-1}. It is noted that the maximum values of $|X_1(\omega)|$ and $|X_2(\omega)|$ are more than a factor three larger than the maximum values of $|X_4(\omega)|$, $|X_5(\omega)|$, $|X_6(\omega)|$ and $|X_7(\omega)|$ indicating that the displacements of the half-cables are much smaller than those of $|X_1(\omega)|$ and $|X_2(\omega)|$. Finally, it is seen that the maximum value of $|X_3(\omega)|$ is significantly larger. This indicates that the displacements of the TMD could be relatively large.

With $\sigma_X = 1$, optimal values of c_0 and k_0 are determined with $\alpha_m = 0{\cdot}1$, $m_0 = 200$ kg and α_F chosen such that the static displacements of the two cables are equal.

The results are for spectra 1 and 2, that the optimal values should be chosen to $k_0 = 1200$ N/m and $c_0 = 15$ N s/m if σ_1^2 is minimized. The corresponding value of the variance is $\sigma_1^2 = 2{\cdot}89$. No minimum is found if σ_2^2 is minimized. The reason is that the main part of the response has frequencies outside the limits of spectra 1 and 2.

For spectrum 3, the optimal damper characteristics should be chosen to $k_0 = 2350$ kg/m and $c_0 = 50$ N s/m if σ_1^2 is minimized and $k_0 = 1600$ kg/m and $c_0 = 210$ N s/m if σ_2^2 is minimized. The corresponding values of the variances are $\sigma_1^2 = 0{\cdot}81$ and $\sigma_2^2 = 4{\cdot}04$. It is noted that Figures 4–10 correspond to the situation where σ_1^2 is minimized.

In order to estimate the effect of the TMD, the total variance of the degrees of freedom X_1 and X_2 is determined if the TMD is removed for load spectrum 3. The result is

$$\sigma_{X_1}^2 + \sigma_{X_2}^2 = 5{\cdot}82 \tag{39}$$

It is noted that when the TMD is not present, the variables X_4–X_7 vanish, since there will not be a discontinuity of the slope of the cables at their midpoints. The value calculated in 39 is, therefore, comparable to the values given in the seventh column in Table 1. Hence, it is seen that when minimizing σ_1^2 for the load case of spectrum 3, the TMD reduces the variance of the cable degrees of freedom with more than a factor seven. The results are summarized in Table 1.

Finally, it should be noted that problems with large displacements of the TMD could be expected if the excitation from the pylons has frequencies larger than 5 s^{-1}. However, in practical applications, this limitation is not expected to be critical.

5. CONCLUSIONS

Twin cables, used in many modern cable-stayed bridges, are sensible to large in-plane vibrations. A passive vibration control of these vibrations is suggested by means of a passive linear viscous mass–damper placed between the cables at their midpoint. The mass–damper is tuned based on a linear model for the motion of the twin cables and the mass–damper. The linearization is justified by the results obtained at optimal design, where a significant reduction in vibration levels is notified. Both the motion of the half-cables, the support point of the TMD and the secondary mass are controlled. The loading consists of random motions of the support point of the pylon, which is modelled as a band-limited white noise process. The sum of the stationary variance of the degrees of freedom of the system is minimized with respect to the spring stiffness and the damper constant. The results showed that the response variances could be reduced below 14% of their uncontrolled values. It should be noted that this performance is calculated from the linear cable response. However, according to [5] the harmonic frequency response functions of the in-plane modal co-ordinate in the nonlinear case is only a little smaller than the corresponding linear one. In any case, the TMD at optimal tuning can reduce the vibrations below the level, where the cable is prone to whirling motions.

ACKNOWLEDGMENT

The present work has been supported by the Danish Technical Research Council within the research program *Damping Mechanisms in Dynamics of Structures and Materials*.

REFERENCES

1. M. Virlogeux, 1998 *Proceedings of the International Symposium on Advances in Bridge Aerodynamics*, *Bridge Aerodynamics*, *Copenhagen*. Cable vibrations in cable-stayed bridges.
2. H. M. Irvine 1981 *Cable Structures*. Cambridge, Massachusetts: MIT Press.
3. C. Verwiebe, 1998 *Proceedings of the International Symposium on Advances in Bridge Aerodynamics*, *Bridge Aerodynamics*. Rotterdam: A. A. Balkema. Rain–wind induced vibration of cables and bars.
4. J. L. Lilien and A. Pinto Da Costa: 1994 *Journal of Sound and Vibration* **174**, 69–90. Vibration amplitudes caused by parametric excitation of cable stayed structures.
5. S. R. K. Nielsen and P. H. Kirkegaard 2002 *Journal of Sound and Vibration* **251**(1), 79–102. Super and combinatorial harmonic response of flexible elastic cables with small sag.
6. C. L. Lee, and N. C. Perkins 1992 *Nonlinear Dynamics* **3**, 465–490. Nonlinear oscillations of suspended cables containing two-to-one internal resonance.
7. Y. K. Lin 1976 *Probabilistic Theory of Structural Dynamics*. Huntington, NY: Krieger Publishing.